Measurement of Angle Distribution in Multiple Scattering by Track Digitization Method (Commemoration Issue Dedicated to Professor Takuji Yanabu on the Occasion of his Retirement)

AUTHOR(S):

Kobayasthi, Shigeharu; Kunitake, Tetsuji; Kitagawa, Katsuya

Bull. Inst. Chem. Res., Kyoto Univ., Vol. 60, No. 2, 1982

Measurement of Angle Distribution in Multiple Scattering by Track Digitization Method

Shigeharu KOBAYASHI, Tetsuji KUNITAKE and Katsuya KITAGAWA

Received April 7, 1982

The multiple scattering of β-ray with neon gas atoms is studied by use of the projection spark chamber. The tracks are digitized and analysed on-line to give the projected angle distribution. The present data are compared with the Molière theory.

KEY WORDS: Angle distribution/ Muliple scattering/ β-ray/ Track digitization/ Molière theory/

1. INTRODUCTION

The study of multiple scattering of charged particles in matter has a long history in both theoretical and experimental approaches. As for the latter, a wide variety of materials or particles has been investigated by many authors.[1~7] Their conclusions were roughly coincided with each other in the relative agreement of their results with Molière theory except for a few cases of the heavy ions.[6,7]

Since these experiments were performed by the incident particles with high momenta bombarded to relatively thick materials, the recent interest may be directed to thinner target and lower incident energy. This is especially important whenever an experiment is concerned with the detection of low momentum particles, which is always accompanied with non-negligible effect of multiple scattering.

In this paper we describe the empirical angle distribution seen in the multiple scattering of β-particle with gaseous neon atoms. Although this is not always aimed to the high quality measurement, the result is compared with that of the Molière theory. We emphasize here that the main purpose of this study is to find the feasibility of on-line processing of a visualized track, since this is anyway the first attempt of phisics experiment relevant to the simple pattern recognition.

2. EXPERIMENTALS

We have been developed a method of particle detection by using a streamer or a spark chamber operated in the projection mode.[10] The visualized particle track was then measured using a video camera and a video digitizing system. We used a solid-state image sensor, having an array of 512(v) $\times$383(h) light sensing elements. Its optical response will be seen in the published paper.[10] The spectral response of the sensor covers the visible wavelength region and extends to the infra-red region. Its maximum

* 小林茂治, 国武哲二, 北川克也: Department of Physics, Saga University, Saga.

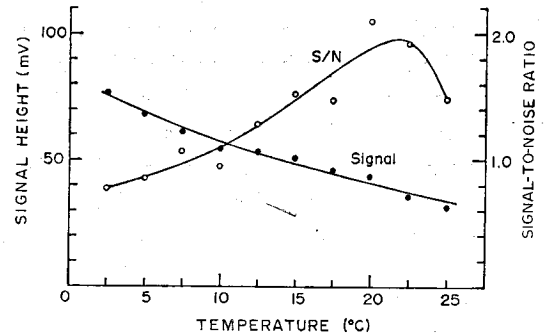

Fig. 1. Temperature dependence of the video signal and of the signal-to-noise ratio for a surface channel type CCD. The illumination over the CCD surface was made by a neon lamp. Each curve is a fit to the measured values by eyes.

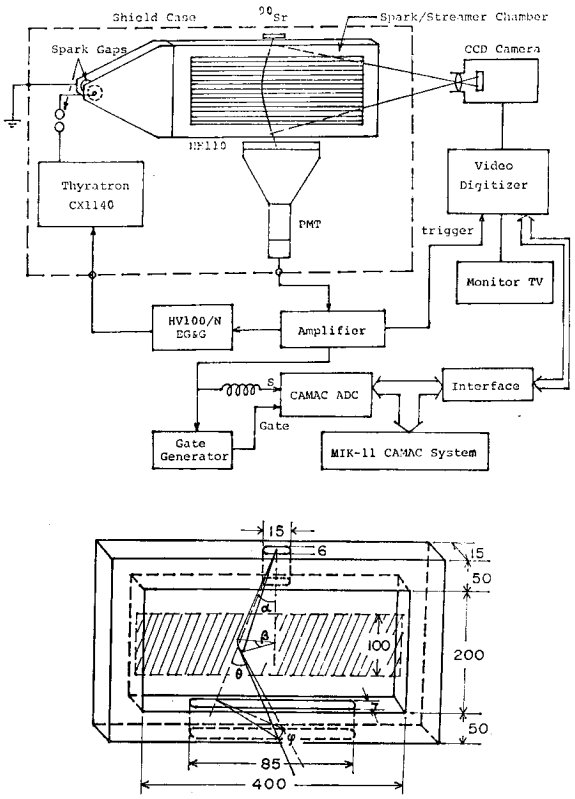

Fig. 2. Schematic of experimental set-up. The trajectory of a particle appearing outside the shaded area in the detail of the chamber was approximated to the separate straight lines and their opening angle was measured.

sensitivity is 0.13 μA/lux.

We used a method of so-called 'fat-zero' to increase the light sensibility instead of cooling the sensor. This is realized by illumination of the device using the light emitting diodes. Present choice of the method is based on the following observation: Since the major part of the image sensor is a charge coupled device (CCD) of surface channel type, it has only a little temperature dependence of signal to noise ratio as shown in Fig. 1. The measurement was performed during the cooling of whole camera system down to 0°C, by taking photographs of video signal on an oscilloscope. The temperature was monitored by a thermister mounted on the glass face of the device. The present result is different from that previously reported,[11,12] since the latter is for the CCD of buried channel type more sensitive to the temperature. For detecting weaker light signal than the present case, the use of buried channel type may be advantageous.

In order to digitize the video signal, we used a digitizer having the memory region of more than 240(v) $\times$256(h) $\times$4(analog) bits, *i. e.* 32 K bytes. This digitizer initially supplied with the S-100 format was modified to be fitted for the CAMAC format. The interfacing from S-100 to CAMAC is illustrated in our paper.[10]

The experimental set-up is as shown in Fig. 2. The main particle detection system is an optical spark chamber and those instruments mentioned above. The particles used here are β-ray from a radio-active source ^{90}Sr. These are detected by a scintillation counter located just beneath the chamber and used for triggering the thyratron pulse. This pulse, before application to the chamber, was shaped by two spark gaps suitably for producing the tracks in projection mode. The pulse hight of the counter signal was measured by an analog-to-digital converter (ADC), and used in determining the energy of β-ray. The digitized track data and ADC data were then analyzed properly using a computer system MIK-11.

3. DATA ANALYSIS

In the present experiment, attension is focussed on the measurement of angular spread for β-ray suffering the multiple scattering with neon gas atoms. The event rate could be adjusted by a dead time controller suitably for the on-line measurement. The data analysis is yet desirable to be as fast as possible, where employed is the data search following the least square fittings of a track to the separate straight lines. The opening angle between the lines is then measured and memorized. At first we programmed such analysis by linking with a CAMAC-handler. With this method the time necessary for the present analysis is as long as 10 sec. We then modified the programme for data search by writing in MACRO language, thereby the time was reduced to about 1/10.

As is mentioned before, the video data amount as large as 30 K bytes per event: to analyse them all is quite inefficient since the track data occupy only a very little portion of whole pictorial area. The method applicable in the present case is to restrict the scanning region as follows: The initial data search is made on whole one line, and then remembering the position of data X_0, the next data search is made for the region of $2\Delta X$ centred at X_0. The absence of data point in some line brings about twice

change in the width for next data search. Such procedure is continued until coming to the predetermined vertical position.

In order to find a track centre in a 'flare' frequently seen, only the points with maximum intensity are searched in each lines. In this experiment, each 5,000 track events for the neon gas data and for the data of acrylate plastic of 2 mm thick were analyzed by this method. After termination of such on-line analysis for the total events, some off-line programmes are started. These are the sorting of vertical intervals (or approximately the path length) remained without search, and that of pulse height data from the counter. These results are used in estimating the number of atomic electrons/ cm^2 and the energy of incident electron. In Fig. 3 the examples of such analysis for neon gas data is demonstrated graphically, where the shaded or labeled area indicates the region used in deriving the scattering angle distribution.

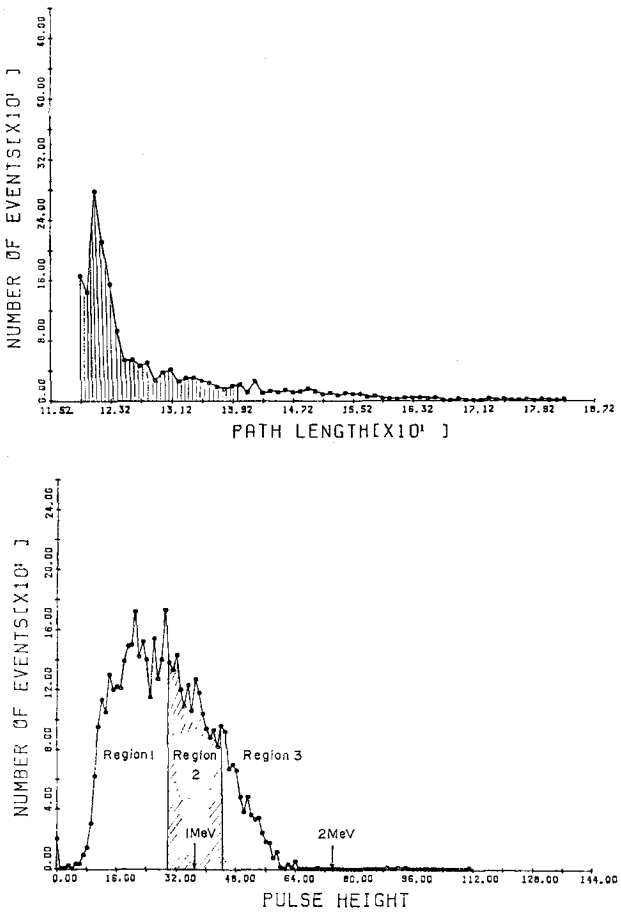

Fig. 3. The path length distribution of β-rays in neon gas, and their energy distribution measured by a ADC. The shaded area indicates the regions used in the analysis.

4. RESULTS

The β-ray emitted from the source is roughly collimated by a slit of 15 mm×6 mm before entering the projection spark chamber having the size of 300×500×15 mm. After scattering with neon atoms, it exits from another slit of 85 mm×7 mm (see Fig. 2). With such a geometry we first computed the acceptance of a particle scattered ideally at one point within the shaded area in Fig. 2.

This calculation is actually based on the two kinds of convolution integrals with respect to the incident angle α for the solid angle element $d\omega(\alpha, \beta)d\omega(\theta, \varphi)$ averaged over the scattering region with and without any acceptance conditions for the present geometry. Denoting the results with $\Delta\omega(\theta)$ and $\Delta\Omega(\theta)$, the acceptance is given by the ratio $\Delta\omega/\Delta\Omega$. The acceptance described as a function of scattering angle θ in Fig. 4, shows the quite characteristic behavior: As seen by an illustration in the figure, the first acceptance cut begins with θ_1. Further increase of scattering angle results the gradual decrease in the acceptance until the beginning of second cut at θ_2, thereafter the acceptance decreases faster.

We used the integrated angle data within each 2° interval, because the number of events presently collected is rather few. The whole energy region is devided into 3 parts, and the angle spread that will be discussed hereafter is mainly on the second region having the energy of 1±0.2 MeV. The raw data in each energy intervals are given in the first 3 figures of Fig. 5. The slight decrease in the width of angle distribution is seen as going towards higher energy regions. Also we can see the wider angular spread for the acrylate data in the last figure of Fig. 5, which is roughly compared with the second data for neon. The acrylate data, however, have something left to be investigated further on account of the possibility of acceptance cut of so many events. Therefore we do not discuss it in more detail.

We note here that these angle distributions should be corrected for the deviation from the actual angle due to the rectangular pixel element (22 μm×26 μm) of image

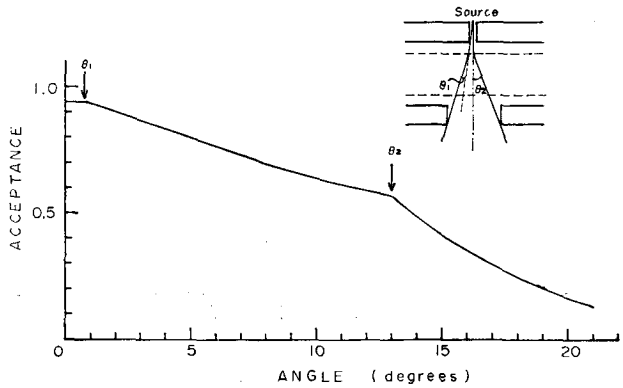

Fig. 4. The calculated acceptance as a function of the projection angle.

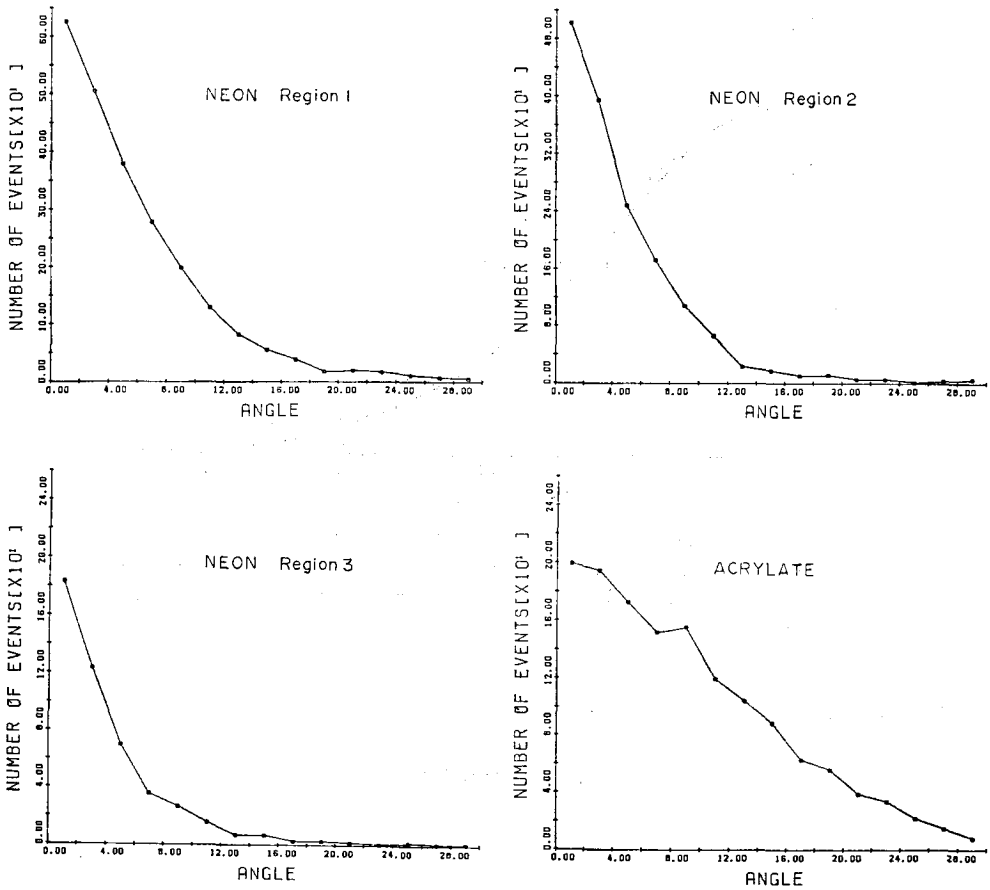

Fig. 5. The uncorrected angle distributions. The first 3 figures are related to the data for neon gas, and the last one is to the data for acrylate plastic layer installed in the chamber. In this case the incident energy was taken as around 1 MeV.

sensor. The calculated relationship between the measured and actual angles happens to show a good linearity. Therefore we have only to make that correction uniformly to the measured angles, which results in the 16.7% increase of these angles. We then integrated above mentioned $\Delta\omega$ and $\Delta\Omega$ for each angular interval, and derived the acceptance to be used in correcting the data. After making such corrections, the corrected number of events were summed up and the result was used in the normalization of angle distribution. This distribution for 1 ± 0.2 MeV electrons is given in Fig. 6. The $1/e$ width of the distribution is 9.7 ± 0.86 degrees, *i e.* the angle at which the distribution falls to the $1/e$ of its maximum value. The error was estimated from the uncertainties of the angle itself and the path length (see eq. 5).

Now we compare the present $1/e$ width with the predicted value from one of the existing theories, the Molière theory. Let us first follow the review article by William Scott[8] for deriving the Molière's distribution function. Therein the critical angle and

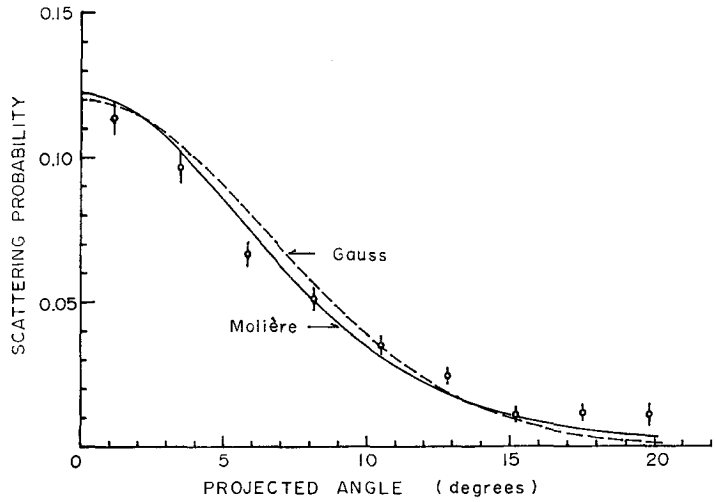

Fig. 6. The corrected angle distributions for 1 ± 0.2 MeV β-rays indicated by the circles. The calculated distribution after the Molière theory is given by the solid curve. The dashed curve represents the first term of the Molière expansion having the gaussian shape.

the Molière's screening angle are respectively given by;

$$\chi_c=\sqrt{4\pi N(Z^2+Z)}\,e^2/pv \qquad (1),$$

and

$$\chi_a=\chi_0\sqrt{1.13+3.76\alpha^2} \qquad (2).$$

Here the Born screening angle χ_0 and his parameter α are defined by;

$$\chi_0=(1.13/137)\,Z^{1/3}mc/p \quad \text{and} \quad \alpha=Ze^2/\hbar v.$$

In these expressions, N is the number of atoms/cm^2, Z the atomic number, m the electron mass, and p and v the incident momentum and velocity, respectively. The Molière's B is a solution of the following equation:

$$B=ln\,B+ln(1.1669\Omega_0) \qquad (3),$$

by using the mean number of collision Ω_0 given by $(\chi_c/\chi_a)^2$. With these parameters, the reduced distribution function $f_{red}(\vartheta)$ is described as;

$$f_{red}(\vartheta)=2/\pi\int_0^a d\eta\,\cos(\vartheta\eta)\,\exp(-\eta^2/4+(\eta^2/4B)\ln(\eta^2/4)) \qquad (4),$$

where the reduced angle $\vartheta=\theta/\chi_c\sqrt{B}$ is defined for an observable projected angle θ. This integral is usually expanded with the power series of $1/B$ and its first term has a gaussian form. Through the calculation of the eq's. 1 to 3, we obtain $B=6.229$ (or $\Omega_0=95$) and $\chi_c\sqrt{B}=9.4°$ for 1 MeV electron's path length of 100 mm in neon gas.

We computed the distribution function $f(\theta)=\chi_c\sqrt{B}f_{red}(\vartheta)$ for $a=10\sqrt{B}$, * which is given by the solid curve in Fig. 6. In the same figure, the gaussian distribution is also presented by the dashed curve. In order to examine the effect on the energy spread in this measurement, we computed also the angle distributions for 0.8 MeV and 1.2 MeV incident electrons. The corresponding $1/e$ widths were 10.2 and 7.5 degrees respectively. Assuming the uniform energy distribution in this energy interval, the theoretical $1/e$ width is resulted in 8.83 ± 0.76 degrees, which is roughly consistent with the measured width.

Then we compare our width with the result from so-called Highland's formula for a simple calculation of $1/e$ width:

$$\theta_{1/e}=E_{sx}/(pv)\sqrt{X}(1+log\,(X)/9) \qquad (5),$$

where X is the thickness of the scatterer measured in radiation length and E_{sx} is a constant in MeV. The value of $E_{sx}=12.7$ MeV in the Highland's paper[9] is found to be inadequate for explaining present data since our value for X is 0.1/321. Recently the value for E_{sx} was modified to 20 MeV.[5,13] By this the $1/e$ angle of eq. 5 is 9.4°, which is consistent with our width even after correcting for the error of 5-10% relevant to the formula.

5. DISCUSSION AND CONCLUSION

We emphasize first the advantage of using the projection chamber[14] in the track visualization. Comparing with an alternative, the streamer chamber, it works with much lower voltage (~10 KV), which means that the detector stability increses and the e-m radiation noise decreases. Moreover the brightness of track is much larger than that for the streamer tracks, and therefore the track digitization is enabled. The merit of using the present apparatus for the multiple scattering experiment is to have an information of angle of incidence, thereby the accurate measurement of scattering angle will be possible.

That the present experiment is not truely warranted in the fine evaluation of the Molière theory is merely on the trivial reasons; the broad energy spectrum of incident particles and rather small particle acceptance of the detector. The empirical result for the projected angle distribution showed, however, the consistency with the Molière theory and the Highland's formula. Anyway the primary purpose for finding the feasibility of processing a visualized particle track is at least attained through the present study.

*: The significant integration limit a should be chosen enough large to be reproduced an expected 'tail' in the angle distribution. We used the value for a ten times larger than that in the Scott's paper[8], because in our case his choice of $a=\sqrt{B}$ was found insufficient.

REFERENCES

(1) L. A. Kulchisky and G. D. Latyshev, *Phys. Rev.* **61**, 254 (1942).
(2) A. O. Hanson, L. H. Lanzl, E. M. Lyman, and M. B. Scott, *Phys. Rev.* **84**, 634 (1951).

(3) H. Bichsel, *Phys. Rev.* **112**, 182 (1958).
(4) E. V. Hungerford *et al.*, *Nucl. Phys.* **A197**, 515 (1972).
(5) G. Shen *et al.*, *Phys. Rev.* **D20**, 1584 (1976).
(6) B. W. Hooton, J. M. Freeman, and P. P. Kane, *Nucl. Instr. Meth.* **124**, 29 (1975).
(7) G. Spahn and K. O. Groeneveld, *Nucl. Instr. Meth.* **123**, 425 (1975).
(8) W. T. Scott, *Rev. Mod. Phys.* **35**, 231 (1963).
(9) V. L. Highland, *Nucl. Instr. Meth.* **129**, 497 (1975).
(10) S. Kobayashi, M. Koga, and Y. Haraguchi, *Nucl. Instr. Meth.* to be published and also in S. Kobayashi and H. Itoh, Proceedings of INS Intern. Symposium on Nuclear Radiation Detectors, 606 (1981).
(11) W. O. Wallik, R. G. Kenyon, and H. J. Lubatti, *Nucl. Instr. Meth.* **146**, 403 (1977).
(12) F. Villa and C. Wang, *Nucl. Instr. Meth.* **144**, 533 (1977).
(13) Particle Data Group, *Rev. Mod. Phys.* **52**, No. 2 (1980).
(14) G. Charpak, A. Breskin, and F. Piuz, *Nucl. Instr. Meth.* **100**, 157 (1972).